Electronic Supplementary Material (ESI) for Nanoscale.

A polymeric temozolomide nanocomposite against orthotopic glioblastoma xenograft: tumor-specific homing directed by nestin

Suma Prabhu[a], Jayant Sastri Goda[b], Srinivas Mutalik[c], Bhabani Shankar Mohanty[b], Pradip Chaudhari[b], Sharada Rai[d], Nayanabhirama Udupa[5] and Bola Sadashiva Satish Rao[a *]

[a] Department of Radiation Biology and Toxicology, School of Life Sciences, Manipal University, Manipal– 576 104, Karnataka, India.

[b] Advanced Centre for Treatment, Education and Research in Cancer, Tata Memorial Centre, Navi Mumbai – 410 210, Maharashtra, India.

[c] Department of Pharmaceutics, Manipal College of Pharmaceutical Sciences, Manipal University, Manipal – 576 104, Karnataka, India.

[d] Department of Pathology, Kasturba Medical College (Mangalore Campus), Manipal University, Mangalore –-575 001, Karnataka, India.

[e] Director - Research (Health Sciences), Manipal University, Manipal – 576 104, Karnataka, India.

***Corresponding Author:** **Prof. B. S. Satish Rao**

Department of Radiation Biology & Toxicology

School of Life Sciences (SLS), Manipal University,

Manipal-576104, Karnataka, India

Tel: +91-820-2922815

Fax: +91-820-2571919

Email: satishraomlsc@gmail.com or rao.satish@manipal.edu

Supplementary Information

1. Chemicals

Poly (lactide-co-glycolic acid) (PLGA) (lactide : glycolode – 50 : 50), bi-functional poly ethylene glycol (COOH-PEG-NH_2), 1-Ethyl-3-(3-dimethylaminopropyl) carbodiimide (EDC) and N-Hydroxysuccinamide sodium salt (NHS), D-α-Tocopherol polyethylene glycol 1000 succinate (TPGS) were purchased from Sigma, USA. HPLC grade solvents such as acetic acid and acetonitrile were purchased from SRL, India. Stannous chloride, DMEM, fetal bovine serum (FBS) and gentamicin (Antibiotic solution) were purchased from Himedia Laboratory, India. TMZ was a kind gift from Strides Acrolabs Pvt. Ltd. Bengaluru, India.

2. Animals and Cell lines

Athymic, immune compromised homozygous BALB/c nude mice and NOD-SCID mice weighing 24.00 ± 2.00 g were used for development of orthotopic glioblastoma xenograft model. Animal experiments and surgical procedures were performed with prior approval from Institutional Animal Ethics Committees, Kasturba Medical College, Manipal University, Manipal for BALB/c nude Mice (Approval no: IAEC/KMC/92/2013) and Tata Memorial Centre, Advanced Center for Treatment, Education and Research in Cancer, Navi Mumbai for NOD-SCID mice (Approval no: IAEC/ACTREC/11/2015). Animal care and handling was done according to the Jacksons Laboratory guidelines for immune deficient mice (https://www.jax.org/jax-mice-and-services/customer-support/technical-support/breeding-and-husbandry-support/special-care). All animals included in the study were maintained with absolute biological containment, in an individual ventilated sterile cages and bedding. Animals were acclimatized to a controlled habitat at controlled temperature (22 ± 3°C), humidity (50 ± 5%) and light (12 h cycle of light and dark) with access to food and water *ad libitum*.

U-251 MG (glioblastoma cells) and its normal counterpart SVG cells (SV40 transfected normal astrocytes / astroglial cells), were a kind gift from Prof. Kumar Somasundaram, Department of Microbiology and Cell Biology, Indian Institute of Science Bengaluru, India. These cells were cultured in DMEM medium supplemented with 1% fetal calf serum (FCS) at a temperature of 37°C, in a CO_2 incubator with 5% humidity. The cells were used for experimentation during the log phase of growth.

We developed glioblastoma orthotopic mouse xenograft model using U-251 MG cells in BALB/c Nude mice (at Manipal University) to evaluate pharmacokinetics. Besides, we also developed orthotopic tumors in NOD SCID mice (at ACTREC), mainly for non-invasive imaging and assessing *in vivo* anticancer efficacy for repeated intravenous injections. Both these animal models are immune deficient wherein, NOD SCID is deficient in T-cells, B-cells and NK-cells, while BALB/c Nude mice are deficient in T-cells, however growth of intra cerebrally implanted tumor did not show any substantial variation in both these models.

3. Development of orthotopic glioma xenograft

Intra cerebral inoculation of cells (U-251 MG) was done as described previously[1] with minor modifications. Briefly, animals were anesthetized by an intraperitoneal injection of Ketamine (50 mg / kg.b.wt.) and Xylazine (5 mg / kg.b.wt.) mixture. Once the animal was adequately anesthetized, it was fixed to the stereotaxic head frame (Stoelting for Mouse™, 51725D, USA). Following skin incision (10 - 12 mm), a burr hole was drilled 2.3 mm to the right and 1 mm posterior to the bregma. Later, 5×10^5 U-251 MG cells in a volume of 5 µl of serum free DMEM were inoculated at a depth of 3 mm using a Hamilton syringe (900 series; USA). The cell

suspension was slowly released at the rate of 0.5 µl / min and left at the site for 2 min post injection to avoid reflux. The needle was drawn out slowly and the skull was sealed with bone wax (Aesculap, USA), and skin was sealed using 3M Vetbond^{TM} collagen tissue adhesive (Santa Cruz Animal Health, USA).

4. Immunocytochemistry

Differential expression of nestin antigen on U-251 MG and SVG cells was determined by fluorescence microscopy and also immunohistochemistry. For immunofluorescence, one lakh cells were seeded on the poly-L-lysine coated cover slips and allowed to attach overnight at 37°C in a CO_2 incubator. After attachment of cells, media was removed and fixed in 10% formaldehyde and processed according to standard IHC world protocol (http://www.ihcworld.com/general_IHC.htm) without permeabilizing the cells. Images were captured using fluorescent microscope (Olympus BX51, Tokyo, Japan). Further, localization of nestin at the site of tumor was confirmed by immunohistochemical staining of intracerebral tumor bearing mice brain according to the standard protocol (http://www.ihcworld.com/general_IHC.htm). The sections were analyzed using light microscope (Nikon Eclipse E200-LED, USA).

5. Determination of Entrapment Efficiency

Entrapment efficiency was determined by estimating the amount of un-entrapped / non-encapsulated TMZ found in supernatant from nano formulate repeated washings by RP-HPLC (Reverse Phase High Performance Liquid Chromatography) (Waters Alliance 2695, USA), using a C-18 column (Eclipse XDB-C18 Column; 4.6 × 250 mm, 5 µm, Agilent Technologies, USA) and a UV detector at 330 nm (Waters 2487, USA). The column was eluted in isocratic mode

using acetonitrile (Sigma, USA) and 0.1% acetic acid (Sigma, USA) at a flow rate of 1 ml/min. TMZ in the supernatant was quantified using a known standard curve of TMZ. Entrapment efficiency and was calculated using the following formula:

$$\text{Entrapment Efficiency} = \frac{Total\ TMZ - TMZ\ in\ supernatant \times 100}{Total\ TMZ}$$

6. Quantification of Transferrin and Anti nestin antibody by RP-HPLC

Quantity of transferrin and anti-nestin Antibody left un-bound to polymeric magnetite nanoparticles in the supernatant and subsequent washes were quantified by RP-HPLC in order to indirectly determine the concentration of proteins bound to the formulation. In this regard, transferrin and antibody were determined by injecting the supernatant in to a C4 column (Grace Vydac 214TP^{TM} , Germany) and detected using a UV detector at 280 nm (Waters 2487, USA). The heated column (65 C) was eluted with a gradient of 0.1% TFA in Acetonitrile and MilliQ (2.5:97.5) (solvent A) and 0.1% TFA in Acetonitrile and MilliQ water (90:10) (Solvent B) for transferrin with a flow rate of 300 µL for 19 min. Antibody was eluted with a gradient of MilliQ : Acetonitrile : Trifluoroacetic acid (90:10:0.05%) (Solvent A) and MilliQ: Acetonitrile : Trifluoroacetic acid (20:80:0.05%) (Solvent B) with a flow rate of 500 µl / min for 45 min (Table S1).

Table S1. Gradient of solvent system for elution of Transferrin and Anti-Nestin antibody

Gradient for transferrin			Gradient for anti-nestin antibody		
Time (min)	**% A**	**% B**	**Time (min)**	**% A**	**% B**
0.0	90	10	0.0	90	10
15.0	30	70	15.0	30	70
15.1	0	100	15.1	10	90
16.0	0	100	25.0	0	100
16.1	90	10	44.0	0	100
19.0	90	10	45.0	90	10

Solvent system for transferrin: Solvent A – 0.1% TFA in acetonitrile and MilliQ water**;** Solvent B – 0.1% TFA in acetonitrile and MilliQ water (90:10)

Solvent system for Antibody: Solvent A – MilliQ water: acetonitrile : trifluoroacetic acid (TFA) (90:10:0.05%); Solvent B – MilliQ water: acetonitrile : TFA (20:80:0.05%)

7. Direct labeling of Technetium 99m (^{99m}Tc) to TMZ / STAT / STAP/STT

Pertechnetate was used to label TMZ and nanocomposites using stannous chloride ($SnCl_2$, HiMedia, India) as a reducing agent. TMZ (1 mg/mL) was dissolved in 0.1% Di-methyl formamide, while, STAT / STAP/ STT were dispersed in 0.9 % saline. Later, 75 µg and 100 µg of $SnCl_2$ (1 mg/mL stock of $SnCl_2$ in 0.1N HCl) was added to the vial containing TMZ and formulation respectively. The pH of these mixtures was adjusted to 6 using 0.5 M $NaHCO_3$ (MERK, India). Further, 1 mCi of ^{99m}Tc was added to this mixture and incubated at room temperature for 40 min. The efficacy of labeling was evaluated by loading 2 µL of the labeled radiopharmaceutical on Instant Thin Layer Chromatographic plate (iTLC, Agilent Technologies, USA), and run using acetone as a mobile phase. The ITLC plate was cut into strips of 1 cm length and each strip was evaluated for the total gamma counts per minute using automated

gamma counter (Perkin Elmer, Wizard 1470 Automatic Gamma Counter, Austria). The labeling efficiency was evaluated using the following formula:

$$\text{Percentage Labeling Efficiency} = \frac{Total\ Counts - Free\ Counts\ \times 100}{Total\ Counts}$$

8. Radiolabelled TMZ, STAT/ STAP / STT

Pure TMZ, STAT and STAP were radiolabelled using ^{99m}Tc using stannous chloride as a reducing agent. The labeling efficiency of TMZ, STAT, STAP and STT was ascertained to be > 87% at pH 6 (Table S2). In order to demonstrate the fate of engineered nanocomposites in systemic circulation, we directly labelled TMZ, STAT, STAP and STT with ^{99m}Tc using stannous chloride. A simple chemistry of reducing pertechnetate ion becomes a prerequisite to label / complex.

Table S2: Labelling efficiency of ^{99m}Tc to pure TMZ, STAT, STAP and STT nanocomposites

pH	$SnCl_2$ (µg/mL)	TMZ	STAT	STAP	STT
6.0	75.00	90.63 ± 2.86	-	-	-
	100.00	-	87.59 ± 2.34	88.25 ± 2.52	88.93 ± 1.12

$SnCl_2$ – Stannous Chloride; All other abbreviations as in Table 1.

9. Validation of Bio-analytical Method for Estimation of TMZ in Plasma and Brain

The methodology of TMZ quantification in plasma and brain was validated according to the standard guidelines by U.S. Department of Health and Human Services (http://www.fda.gov/downloads/drugs/guidancecomplianceregulatoryinformation/guidances/ucm368107.pdf). Briefly, animals (n = 3) were anesthetized with Ketamine (50 mg / kg.b.wt.) and Xylazine (5 mg / kg.b.wt.), and blood was collected by retro-orbital bleeding into a heparinized tube, after which they were euthanized to excise the brain. Heparinized blood was centrifuged at

1398 g for 10 min and plasma was separated, collected in Eppendorf tubes and spiked with varying concentrations of TMZ (0.1, 0.5, 1, 2, 5, 10, 15 µg/ml), parallel with an internal reference standard theophylline (I.S. – Internal Standard with a structure similar to that of TMZ) in separate aliquots. This was further acidified with 0.1N HCl (3 µL / 100 µL plasma). Brain tissue was homogenized using phosphate buffered saline (PBS) and tissue homogenate (10 %) was made. This homogenate was also spiked with TMZ and theophylline as separate aliquots and acidified with 0.1N HCl (500 µL / mL of homogenate). Spiked TMZ and theophylline were extracted by ethyl acetate extraction method as described earlier. [3] Linearity was determined by a standard calibration curve of AUC (Area under the curve) ratio of TMZ to IS against the nominal concentration of TMZ. Based on this highest limit of quantification (HLQ), mid limit of quantification (MLQ) and lowest limit of quantification (LLQ) were assessed for their accuracy, recovery and precision. As per CHMP guidelines, (http://www.ema.europa.eu/docs/en_GB/document_library/Scientific_guideline/2011/08/WC500109686.pdf) the mean concentration for accuracy and precession should be within 15% of the nominal values for the QC samples, except for the LOQ which should be within 20% of the nominal value.

10. Bio-analytical Validation of TMZ in Plasma and Brain Tissue Homogenate

Quantification of drug is of a paramount significance for validation of any clinical products. Outcome of the animal toxicokinetics plays a crucial role in resolution of efficacy and safety of the product. Thus our study validated and documented a satisfactory standard yielding authentic results (Table S3, S4 and S5). We validated the quantification method by measuring linearity, precession, recovery, accuracy, LOD (limit of detection) and LOQ (limit of quantification), keeping standard reference values

(http://www.fda.gov/downloads/drugs/guidancecomplianceregulatoryinformation/guidances/uc368107.pdf) judging the quality of assay.

Table S3. Precession of TMZ estimation in plasma and brain homogenate spiked with low, medium and high quality control samples

Precession	**Plasma (%)**		**Brain (%)**	
	Day 1	Day 2	Day 1	Day 2
HLQ	13.83	10.14	13.07	13.57
MLQ	13.60	11.52	14.84	12.93
LLQ	14.69	13.81	09.81	13.99

HLQ: Highest limit of quantification**; MLQ:** Mid limit of quantification**; LLQ:** Lowest limit of quantification.

Table S4. Accuracy of plasma and brain homogenate spiked with low, medium and high quality control samples of TMZ

Accuracy (%)	**Plasma (%)**			**Brain (%)**		
	HLQ	MLQ	LLQ	HLQ	MLQ	LLQ
80	12.75	13.37	18.73	06.09	14.78	10.19
100	14.74	13.90	20.41	12.63	05.04	13.72
120	12.06	10.54	19.12	09.23	11.94	07.12

HLQ: Highest limit of quantification**; MLQ:** Mid limit of quantification**; LLQ:** Lowest limit of quantification.

Table S5. Recovery of TMZ from plasma and brain homogenate spiked with low, medium and high quality control samples

	Plasma (%)	**Brain (%)**
Recovery	98.30	101.24
LOD	18.93	18.79
LOQ	17.38	16.94

LOD - limit of detection; **LOQ** - limit of quantification

11. *In vitro* release of TMZ from STAT and STAP

In vitro release of TMZ from STAT and STAP was determined using phosphate buffered saline (PBS) at a pH of 7.4. STAT and STAP (at a concentration of 1mg / mL) was suspended in10 mL of PBS and maintained at 37°C at 50 RPM continuously. The buffer (500 µL) was withdrawn at given time intervals and centrifuged at 11,950 × *g* for 10 min. The supernatant was quantified using HPLC for TMZ according to the protocol mentioned (Materials Section 4.3).

In vitro release profile of TMZ from STAT and STAP demonstrate a sustained and prolonged time dependent release from the nanocomposites. This release profile is concordant with our *in vivo* studies with an increased half-life ($t_{1/2}$) of TMZ. Following an initial release of approximately 20%, both STAT and STAP showed a controlled release, however, STAP showed a decline in TMZ content after 48 h (Fig. S1). Rate limiting release of drug can be attributed to either diffusion from the polymer matrix, penetration of solvent or erosion of the polymeric structural integrity leading to diffusion of TMZ. [4] The release pattern demonstrated in our study exhibited a non-zero ordered kinetics, which can be attributed to hydrolysis of polyester bonds of PLGA.[5] Furthermore, surface modifications in order to enhance stability and shelf life and protein coatings to target tumor cells poses additional criteria for controlled degradation of the polymer and in turn release TMZ.[5] Our hypothesis, is supported by a study wherein trimethylated chitosan surface coatings on PLGA permeabilized the formulation across BBB and prolonged the release of drug.[6] A decline in the release of TMZ from STAP at 48 h might be ascribed to the amorphous feature of the structure. Amorphous nanoparticulate system is generally preferred to enhance bioavailability of poorly water soluble drugs. The polymer molecular chain describes

the degree of crystalline regions in relation to that of the amorphous regions ascribing an important criterion in drug release as the amorphous regions are permeable and accessible to water molecules.[7] The crystallinity and amorphous nature of PLGA depends on the ratio of LA and GA, wherein an 50:50 ratio of LA and GA attributes to the amorphous nature of polymer.[8] Furthermore, the drug release behavior from the polymer is greatly influenced by the physicochemical properties such as molecular weight, LA and GA ratio, end group capping, additives (surfactants / salts), size and shape, porosity and density of the nanoparticulate system.[9] In case of STAP, the nanocomposite comprises of a polysorbate-80 coat. The *in vitro* drug release profile from STAP demonstrated to be influenced also by polysorbate-80 due to enhanced wettability prompting faster release of drug attributing to higher hydrophilicity.[10] Taken together, influence of polymer and surfactant, reduced size of the particle along with a greater surface area and amorphous nature of the polymer embedding TMZ plausibly led to faster release of drug *in vitro* and subsequent indication in sustained and / or decline in the release of TMZ.

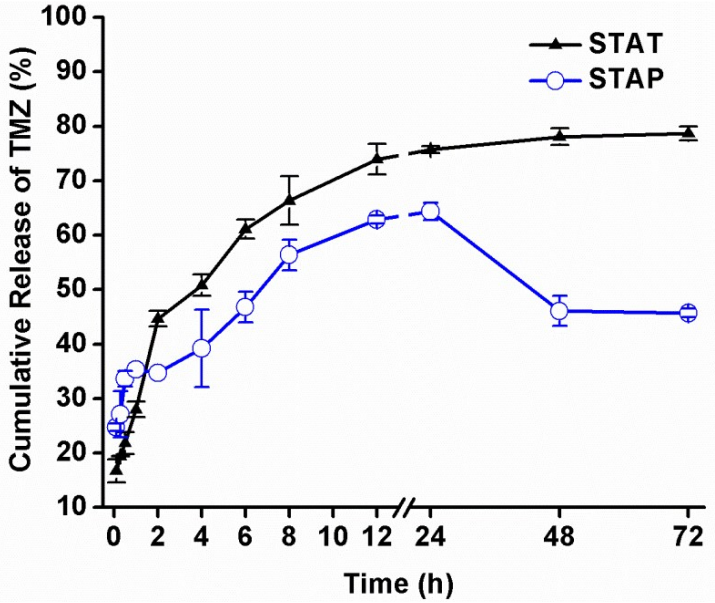

Fig. S1. *In vitro* release profile of TMZ from STAT and STAP at pH 7.4 (values are mean ± SD of three trials).

12. Table S6. Distribution of ^{99m}Tc labelled pure TMZ / STAT / STAP / STT in different organs at different time points *($^{***}p<0.001$ $^{**}p<0.01$, $^{*}p<0.05$ in comparison to TMZ. STT comparison with TMZ: Non-significant).*

Treatment Group	Counts (% ID / cc)	0.5 h	1 h	3 h	5 h	24 h
TMZ	Heart	5.51 ± 1.14	5.88 ± 1.51	3.20 ± 1.26	2.80± 1.45	0.10 ±0.03
	Lungs	9.00 ± 3.65	12.21 ± 3.20*	7.58 ± 3.12	8.06 ± 4.17	0.15 ± 0.04
	Stomach	11.20 ± 1.35***	7.63 ± 0.56 ***	4.65 ± 1.37	1.40 ± 0.03	0.07 ± 0.02
	Liver	68.75 ± 4.69	84.76 ± 12.95	61.29 ±14.09	40.95 ± 14.46	1.19 ± 0.27
	Intestine	10.86 ± 2.88*	8.43 ± 2.50*	11.92 ± 5.49	5.96 ± 2.40	0.09 ± 0.06
	Kidney	22.19 ± 4.11**	20.98 ± 4.84**	16.74 ± 5.54	7.42 ± 3.49	0.15 ±0.02
	Bladder	222.19 ± 96.01	182.30 ± 77.06	101.58 ±97.73	82.37 ± 74.04	0.02 ± 0.05
STAT	Heart	3.54 ± 0.51	1.75 ± 0.08	1.21 ± 0.19	1.28 ± 0.05	0.31 ±0.18
	Lungs	1.28 ± 0.15	1.13 ± 0.08	1.58 ±0.16	1.59 ± 0.10	0.36 ±0.20
	Stomach	1.57 ±0.18 *	1.47 ± 0.21	1.24 ± 0.20	0.82 ± 0.41	0.35 ±0.31
	Liver	106.69 ± 37.71	83.12 ± 24.81	43.64 ± 24.98	33.02 ± 15.70	2.18 ±0.62
	Intestine	0.81 ± 0.24	1.35 ± 0.25	1.15 ± 0.04	1.40 ± 0.15	0.27 ±0.11
	Kidney	5.49 ± 0.83	3.77 ± 1.54	4.73 ± 0.58	4.07 ±1.40	0.12 ±0.04
	Bladder	92.54 ± 2.02	85.38 ± 25.24	32.19 ± 16.82	41.57±21.23	0.21 ±0.05
STAP	Heart	2.45 ± 0.90	2.15 ± 0.82	1.93 ±0.62	0.80 ± 0.10	0.18 ± 0.09
	Lungs	5.25 ± 0.29	3.59 ± 0.90	1.60 ± 0.46	0.81 ± 0.13	0.27 ± 0.17
	Stomach	2.35 ± 0.71 *	2.66 ± 0.59	1.99 ± 0.39	1.01 ± 0.26	0.39 ± 0.17
	Liver	128.23 ±45.69	103.24 ± 15.55	89.84 ± 21.13	54.54 ± 27.12	7.06 ± 0.45
	Intestine	1.06 ± 0.118	1.33 ± 0.78	0.79 ± 0.29	4.98 ± 2.40	0.54 ± 0.30
	Kidney	5.89 ± 2.67	4.73 ± 1.99	4.83 ± 2.34	3.21±1.00	0.44 ± 0.24
	Bladder	63.55 ± 33.09	56.78 ± 26.22	36.56 ± 34.51	12.08 ±9.28	0.23 ±0.10
STT	Heart	2.20 ± 0.62	3.09 ± 0.17	0.97 ± 0.15	1.24 ± 0.40	0.15 ± 0.00
	Lungs	3.54 ± 0.49	2.83 ± 0.50	3.03 ± 0.07	1.39 ± 0.89	0.19 ± 0.05
	Stomach	4.17 ± 0.70	4.38 ± 0.90	4.03 ± 0.60	1.46 ± 0.26	0.39 ± 0.10
	Liver	145.94 ± 21.19	197.77 ± 37.14	123.76 ±18.20	50.51 ± 9.64	1.70 ± 0.85
	Intestine	4.22 ± 0.36	7.00 ± 0.89	4.53 ± 1.44	4.20 ± 1.22	0.34 ± 0.09
	Kidney	10.96 ± 2.22	33.54 ± 2.70	12.98 ± 8.73	11.32 ± 0.87	0.16 ± 0.05
	Bladder	258.45 ± 8.30	216.45 ± 6.42	79.72 ± 1.48	59.49 ± 9.01	0.70 ± 0.56

11. Table S7. Distribution of ^{99m}Tc labeled pure TMZ / STAT / STAP / STT in brain tissue and in tumor at different time points *($^{***}p<0.001, ^{**}p<0.01, ^{*}p<0.05$ in comparison to TMZ. $^{\#}p<0.001$, $^{\$}p<0.01$ when STT in tumor was compared to STAT in tumor).*

Treatment Group	Counts (% ID / cc)	0.5 h	1 h	3 h	5 h	24 h
TMZ	Tumor	0.35 ± 0.06	0.35 ± 0.01	0.11± 0.02	0.08 ± 0.02	5.07E^{-8} ± 1.01E^{-8}
	Brain	9.32 ± 3.76	7.55 ± 3.09	1.76 ± 0.38	1.45 ± 0.21	0.04 ± 0.01
STAT	Tumor	8.87 ± 0.41$^{***\#}$	11.95 ± 1.33$^{***\#}$	4.23 ± 0.56$^{***\#}$	2.81 ± 0.84$^{*\$}$	0.10 ± 0.02*
	Brain	2.71 ± 0.72	2.10 ± 0.57	1.23 ± 0.59	0.44 ± 0.19	0.08 ± 0.06
STAP	Tumor	2.29 ± 0.75**	1.70 ± 0.33**	1.05 ± 0.46**	0.52 ± 0.02*	0.06 ± 0.01*
	Brain	0.35 ± 0.16	0.46 ± 0.16	1.03 ± 0.05	0.00 ± 0.10	0.00 ± 0.00
STT	Tumor	0.63 ± 0.12	0.89 ± 0.03	0.40 ± 0.10	0.01 ± 0.00	0.01 ± 0.00
	Brain	4.30 ± 0.36	7.21 ± 1.18	4.15 ± 0.83	1.25 ± 0.34	0.16 ± 0.04

13. Histopathology of Liver, Spleen and Kidney of Animals Treated with TMZ, STAT and STAP

Liver, kidney and spleen of the animals treated with TMZ, STAT and STAP for *in vivo* tumor response study were harvested, considering the bio-distribution results (Fig. 9). The harvested tissues were fixed in 10% formaldehyde. The fixed tissues were processed and stained with hematoxyline and eosin according to standard protocol. Pathological changes were observed at 40 X magnification using optical microscope (Nikon IX71, Japan). As demonstrated by microSPECT/CT analysis, TMZ, STAT and STAP were found to be deposited majorly in liver, kidney and spleen. In this regard, we performed a microscopic examination of liver, kidney and spleen in all the animals treated with TMZ, STAT and STAP for tumor regression studies to analyze drug induced pathological changes. The group of animals exposed to pure TMZ indicated mild hepatocellular choleostasis, Kupffer cell hyperplasia accompanied by focal necrosis or inflammation leading to congestion in portal triad and dilated sinusoids. However, animals exposed to STAT and STAP indicated mild inflammation and Kupffer cell hyperplasia

(Table S-6). Inflammation and increased sinusoidal space in liver sections may be attributed to drug induced distortion of hepatocyte plasma membrane and lysosomal activity leading to vacuolar degeneration of cytoplasm leading to necrosis.[11] Kidneys did not demonstrate any significant nephrotoxicity, while mild increase in glomerular cellularity was observed in TMZ treated group (Table S-7). Sections of spleen showed large number of megakaryocytes, indicating extramedullary hematopoiesis [11-12] and red pulp congestion due to TMZ and STAP treatment, whereas, STAT treatment did not exhibit much toxic reaction (Table S-8). Representative histopathology photomicrographs have been depicted in Fig. S-2. Thus, STAT was proven to be least toxic, wherein TMZ had been embedded in a complex polymeric construct, in contrast to TMZ direct insult of pure TMZ.

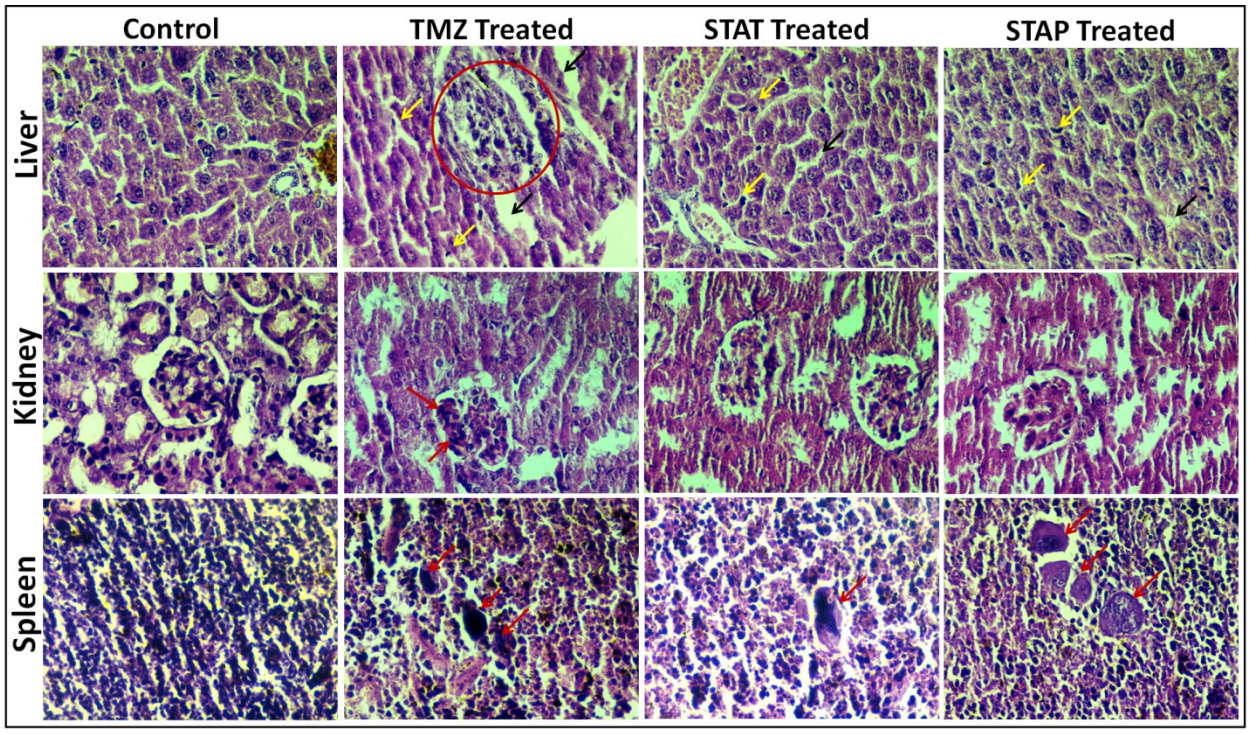

Fig. S2. Representative histopathology photomicrograph of the animals treated with TMZ, STAT and STAP.

The top panel shows the liver sections where, the section of TMZ treated liver shows higher toxicity in comparison to STAT and STAP demonstrating necrosis (red circle), Kupffer cell hyperplasia (yellow arrow) and sinusoidal dilation (black arrow). The middle panel shows sections of kidney showing mild glomerular congestion / cellularity due to TMZ treatment (red arrow), no pathological changes were observed in STAT and STAP treatment. Bottom panel shows spleen section, whereas TMZ and STAP treatment showed increased megakaryocytes (red arrow) in contrast to STAP treatment.

Table S8. Pathology score for drug induced hepatocellular toxicity

Group	Focal Necrosis	Hepatocyte duct destruction	Sinusoidal dilation	Steatosis	Heaptocyte Rosette	Lobular disarray	Choleostasis	Hepatoplasia	Kupffer cell hyperplasia
Control	---	---	---	---	---	---	---	---	+--
TMZ	++-	---	+++	---	---	+--	+++	---	+++
STAT	---	---	+--	---	---	---	---	---	+--
STAP	---	---	+--	---	---	---	---	---	++-

+++ Severe; ++- Moderate; +-- Mild; ---Nil

Table S9. Pathology score for renal toxicity

Group	Tubular necrosis	Tubulointerstitial nephritis	Papillary necrosis	Striped fibrosis	PCT/DCT dilation	Fibrosis /atrophy	Necrosis
Control	---	---	---	---	---	---	---
TMZ	---	++-	---	---	---	---	---
STAT	---	---	---	---	---	---	---
STAP	---	---	---	---	---	---	---

+++ Severe; ++- Moderate; +-- Mild; ---Nil

Table S10. Pathology score for toxicity of spleen

Group	Anisokaryosis	Acidophilic cytoplasm	Megakaryocyte	White Pulp hyperplasia	Red pulp extramedullary hematopoiesis
Control	---	---	---	---	---
TMZ	+--	---	+++	---	+++
STAT	---	---	+--	---	+--
STAP	---	---	++-	---	+--

+++ Severe; ++- Moderate; +-- Mild; ---Nil

References

1. G. A. Mohammed, S. Tejas, C. P. Mark, C. S. Adrienne, *J, Visualized Exp.,* 2011, **57**, e3403.

2. H. Spies, H. J. Pietzsch. Stannous chloride in the preparation of ^{99m}Tc pharmaceuticals. In *Technetium-99m Pharmaceuticals*, Springer, 2007, pp 59-66.

3. E. Gilant, M. Kaza, A. Szlagowska, K. Serafin-Byczak, P. J. Rudzki. *Acta Pol. Pharm. (Engl. Transl.)*, 2011, **69**, 1347-1355.

4. R. A. Jain, C. T. Rhodes, A. M. Railkar, A. W. Malick, N. H. Shah, *Eur. J. Pharm. Biopharm.,* 2000, **50**, 257-262.

5. J. Siepmann, K. Elkharraz, F. Siepmann, D. Klose, *Biomacromolecules,* 2005, **6**, 2312-2319.

6. Z. H. Wang, Z. Y. Wang, C. S. Sun, C. Y. Wang, T. Y. Jiang, S. L.Wang, *Biomaterials,* 2010, **31**, 908-915.

7. G. Odian, *J. Polym. Sci. A Polym. Chem.,* 1991. 768pp

8. G. W. Ehrenstein, *Polymeric materials: structure, properties, applications*, Carl Hanser Verlag GmbH Co KG, 2012.

9. N. Kamaly, B. Yameen, J. Wu and O. C. Farokhzad, *Chem. Rev.,* 2016, **116**, 2602-2663.

10. L. Pachuau and B. Mazumder, *Int. J. Pharm. Tech. Res.,* 2009, **1**, 966-971

11. A. Awaad, *The Journal of Basic & Applied Zoology,* 2015, **71**, 32-47.

12. A. Al-Bader, T. Mathew, M. Khoursheed, S. Asfar, H. Al-Sayer, H. Dashti, *Anat. Histol. Embryol.,* 2000, **29**, 3-8.